Journal of Civil Engineering and Construction 2025;14(4):200-218
https://doi.org/10.65720/jcec.2025.14.4.200

Drifting Behavior of Organic Debris Clouds and Their Interaction with Flow Structures in Mountainous Navigable River Channels

Geng Li[1,2], Jianzhuang Chen[1], Ziyue Zhu[3], Jianghua Liao[4],Jiang Hu[1]*, Shengfa Yang[1]*

[1]*National Engineering Research Center for Inland Waterway Regulation, Chongqing Key Laboratory of Ecological Waterway, Chongqing Jiaotong University, Chongqing, China*
[2]*Department of Civil and Environmental Engineering, University of Missouri, Columbia, MO, USA*
[3]*Department of Civil and Environmental Engineering, University of Virginia, Charlottesville, VA, USA*
[4] *School of River and Ocean Engineering, Chongqing Jiaotong University, Chongqing 400074, China*
E-mail: hujiang1977@cqjtu.edu.cn (Corresponding author), ORCID: https://orcid.org/ 0009-0001-4275-4957.

Received: 08 November 2025; Accepted: 27 December 2025; Available online: 31 December 2025

Abstract: Navigable river channel construction increasingly emphasizes balance of ecological sustainability and waterway transportation. Dike structures are widely applied as they enhance habitat complexity and promote nutrient cycling, yet the mechanisms governing organic debris advection, dispersion, and cloud diffusion in complex hydrodynamics remain unclear. This study focuses on Chaotianmen–Fuling reach of the upper Yangtze River to investigate flow structures and the diffusion behaviors of floating leaves and their grouped clouds within engineered habitats between dikes. Settling experiments on eight common leaf species in static water were first conducted, followed by flume tests and three-dimensional hydrodynamic simulations under different dike configurations. In addition, the leaf drifting process in a natural river was simulated using a Euler–Lagrange approach. Results indicate that recirculation zones with a length-to-width ratio of 3:1 optimize leaf retention, while increased channel constriction enhances turbulence and leaf entry into pools; submerged bars reduce retention efficiency. Moreover, numerical simulation revealed that turbulence and secondary circulation accelerate dispersion of both floating debris and granular clouds, whereas dikes create localized retention zones forming nutrient-rich microhabitats. Application to the real fluvial reach confirmed that the proposed design-channel constriction ratio of 0.33 and bar spacing three times the bar length-improves retention and aggregation of organic and granular matter. These findings provide a scientific basis for integrating habitat restoration with navigation channel construction, offering a model for ecological waterway development in large rivers.
Keywords: River ecological navigation; Leaf transport; Floating debris diffusion; Granular cloud dispersion.

1. Introduction

Rivers, as crucial natural ecosystems, exhibit interactions between hydrodynamic structures and geomorphic forms that profoundly influence mass transport and habitat change. In mountainous rivers, the shoal-pool sequence is an important riverbed geomorphic scheme, typically formed by local variations in bed elevation. The spur dikes (or shallow bar, submerged weir) constrict and guides the flow, while downstream, flow separation and energy dissipation create a relatively low-velocity pool area. This alternating shoal-pool structure not only shapes the morphological diversity of the river but also provides critical habitats for feeding, shelter, and spawning for aquatic organisms such as fish. However, existing research predominantly focuses on the hydrodynamic structure of shoal-pool habitats and direct assessments of their suitability for fish, leaving significant gaps in the understanding of the transport of organic derbies. Thes debris, such as leaves, their processes of deposition, decomposition, and release within pools are vital components of aquatic nutrient cycling and fish food webs.

Spur dikes and similar structures serve as primary means for creating artificial shallow ridge-deep pool systems, and considerable progress has been made in researching the flow field structure around them. Chen experimentally studied the turbulence intensity and flow structures generated in the recirculation zone, and performed detailed measurements of the flow characteristics in the dike recirculation zone, preliminarily revealing the flow patterns around spur dikes [1]. Furthermore, Bai investigated the hydrodynamic characteristics of flow around non-submerged spur dike groups using three-dimensional Large Eddy Simulation (LES), further elucidating the influence of dike length and spacing on turbulent structures. Although the hydrodynamic characteristics of single

or double spur dikes have been relatively well clarified by the studies, research on the hydrodynamic interactions within series of shallow ridge-deep pools formed by continuous multiple spur dikes remains relatively insufficient [2]. On the other hand, studies on sediment transport and deposition in shallow ridge-deep pool systems are relatively abundant. For example, Yang explored the influence of flow turbulence on the sediment-carrying capacity in the recirculation zone downstream of spur dikes [3]. However, organic floating matter such as leaves differs significantly from sediment particles in terms of density, shape, and dynamic response. The movement patterns, distribution characteristics, and retention mechanisms of such material within the complex flow field of shallow ridge-deep pool systems are not yet clearly understood. In summary, while existing research has elucidated the physical habitat functions of shoal-pool systems for fish and accumulated knowledge on their hydrodynamic environment, the following key questions remain: the flow field structure of shoal-pool systems formed by consecutive spur dikes is not yet clear, and the transport characteristics of leaves within such shoal-pool areas remain to be fully understood.

To address the research gaps, we propose a systematic study on the drifting behaviors of organic debris, typically leaves, in mountainous rivers and near the dike groups. The features of the research design include: Investigating the settling mechanisms and key parameters (density, settling velocity) of common tree leaves in the upper reaches of the Yangtze River. Second, through flume experiments considering multiple factors (river width contraction ratio, rifle spacing, submergence level), combined with FLOW-3D numerical simulation and Tracker image processing, the study elucidates how flow field structures (velocity field, turbulent kinetic energy field, recirculation zones) regulate leaf transport. Third, based on the Lagrangian particle tracking method, it quantifies the motion characteristics of leaves before and after implementing the habitat enhancement scheme in the mid-riffle reach, thereby validating the ecological effectiveness of the scheme. Focusing on the riffle-pool habitat in the Chaotianmen to Fuling reach of the upper Yangtze River, this study integrates physical experiments, numerical simulations, and field validation to establish a research framework of "leaf settling characteristics, laboratory flow field and transport experiments, prototype river application and verification," demonstrating experimental feasibility.

This article begins by examining the settling behavior of leaves through controlled experiments, identifying key drivers of deposition, density variation patterns, and settling velocity characteristics, which serve as fundamental parameters for subsequent modeling. Then we integrate generalized multifunctional flume experiments with FLOW-3D numerical simulations to investigate the change of flow structures within the circulation zone under different shoal–pool configurations. Finally, a case study of numerical leave tracking is processed in a reach of the Upper Yangtze River. We simulate three-dimensional flow fields and leaf cloud movement before and after implementing habitat construction schemes, thereby assessing the effectiveness of optimized design parameters in practice. Through this research, we elucidate the regulatory mechanisms by which shoal–pool flow structures influence leaf cloud transport, propose scientifically grounded strategies for habitat optimization, and provide technical and theoretical support for green ecological waterway development in the upper Yangtze River.

2. Materials and Methods

2.1 Experimental Materials

For this experiment, eight leaf types with varying sizes and shapes-Osmanthus, Ficus virens, and Ficus microcarpa-were selected to conduct a preliminary study on the settling characteristics of leaves in the upper reaches of the Yangtze River. Among them, four types were green and four were brown-yellow. All leaves were collected from a river section in Jiangbei District, Chongqing, located in the upper Yangtze region, and were all freshly and naturally abscised (Fig. 1).

The experiment utilized a multifunctional flume with a slope of 1‰ (length 26.5m × width 2.0m × depth 1.0m). The inlet employed reverse-flow steady-state technology, solving the problem of inlet instability in large-scale, high-flow flume experimental systems. The flume outlet was equipped with an adjustable flap gate, which could control the water depth during experiments and ensure smooth and uniform flow conditions (Fig. 2).

Other experimental equipment included an Acoustic Doppler Velocimeter (ADV), high-definition camera equipment (50 Hz), a high-precision electronic balance, a vernier caliper, FLOW-3D numerical simulation software, Tracker video processing software, Python programming tools, etc [4].

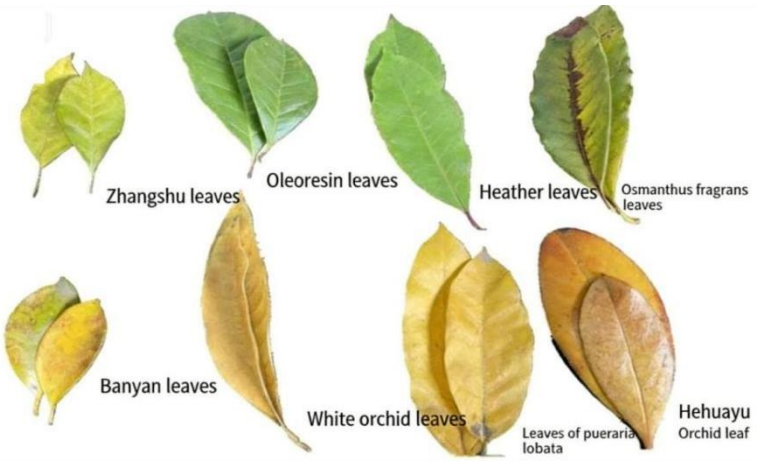

Fig. 1 Typical Leaf Types from the Upper Yangtze Rive

Fig. 2 Multifunctional Flume

2.2 Numerical Model

2.2.1 Numerical Simulation of Flow Field

FLOW-3D software was used to simulate the three-dimensional hydraulic characteristics of the flow field, solving for time-averaged velocities based on the Reynolds-Averaged Navier-Stokes (RANS) equations. Currently, the Navier-Stokes governing equations, primarily composed of the continuity equation, momentum equation, and energy equation, are used to handle complex three-dimensional fluid flows. The Reynolds-averaged N-S equations are as follows:

$$\frac{\partial U_i}{\partial x_i} = 0 \quad (1)$$

$$\frac{\partial U_i}{\partial t} + U_j \frac{\partial U_i}{\partial x_j} = G_i + \frac{1}{\rho}\frac{\partial}{\partial x_j}\left[-p\delta_{ij} + \rho v_T \left(\frac{\partial U_i}{\partial x_j} + \frac{\partial U_j}{\partial x_i}\right) - \rho\overline{u_i u_j} \right] \quad (2)$$

Here, Ui denotes the Reynolds-averaged velocity components in the three spatial directions (i=1, 2, 3 and j=1, 2, 3); Gi is the gravity acceleration term, P is the fluid pressure; v t is the eddy viscosity; and $\rho\overline{u_i u_j}$ corresponds to the Reynolds stresses [5].

2.2.2 Numerical Simulation of Leaves

Based on self-written Python Lagrangian particle tracking code, combined with leaf settling characteristic parameters (density, settling velocity probability distribution) and hydrodynamic data, the transport and settling processes of leaves in the river channel were simulated. The Lagrangian method was employed to track leaf movement, treating leaves as mass points and assigning them the density and settling velocity probability distribution characteristics obtained from experiments. Finally, MATLAB software was used for post-processing to obtain visual results [6].

2.3 Experimental Design and Methods

2.3.1 Experimental Study on Leaf Settling Characteristics

Groups of 16 leaves of different sizes from the 8 species were used, with 10 groups tested. The initial weight and volume of the leaves were measured. Leaves were gently placed on the water surface, and the time from floating to the onset of sinking was recorded. The sinking velocity was calculated in combination with water depth. Finally, the weight of the leaves after settling was measured.

2.3.2 Study on Flow Field Structure and Leaf Transport Characteristics in Shallow-Bar and Deep-Pool Areas

Michelia alba leaves, common in the upper Yangtze, were selected as the experimental subject. Each test condition was repeated 5 times, with 80 leaves released each time. The experiment used a multifunctional flume with a 1‰ slope (length 26.5m × width 2.0m × depth 1.0m). The inlet employed reverse-flow steady-state technology, and the outlet was equipped with a flap gate to control water depth and flow conditions [7].

Based on measured hydrological data from the Zhongdui reach and geometric similarity criteria (Table. 1), experimental parameters were determined: a representative channel width of 800m, horizontal scale of 400, planimetric scale of 20, with leaves not scaled down. Referring to the habitat creation scheme for the Zhongdui reach, experimental bar parameters were set: length 0.66m (channel constriction ratio 0.33), width 0.105m, height 0.1m, bar spacing 2m (three times the bar length) [8].

Table. 1 Measured Hydrological Data from Zhongdui

Discharge（m/s)	Measured Water Level（m)	Water Depth Before Bar（m)	Relative Water Depth
7670	149.48	10.48	0.81
13700	152.63	13.63	1.05
17800	154.03	15.03	1.16
21600	156.32	17.32	1.33
28600	159.28	20.28	1.56
32400	160.96	21.96	1.69
8340	149.94	10.94	0.84
13100	152.44	13.44	1.03
17800	154.43	15.43	1.19
21600	156.19	17.19	1.32
27800	158.72	19.72	1.52
32100	161.24	22.24	1.71
8420	152.30	13.30	1.02
13900	153.27	14.27	1.10
17500	155.05	16.05	1.24
21300	156.94	17.94	1.38
27400	159.25	20.25	1.56
30700	160.86	21.86	1.68
8320	151.58	12.58	0.97
13100	153.69	14.69	1.13
17500	155.29	16.29	1.25
22000	158.35	19.35	1.49
23500	158.36	19.36	1.49
30900	160.91	21.91	1.69

Conditions were designed by varying the channel constriction ratio (0.25, 0.33, 0.50), bar spacing (1.5 times, 3 times bar length), and bar submergence degree (H/D=1.2, 1.5, 1.8). Discharge was adjusted according to conditions to ensure water pressure on the flume sidewalls remained within acceptable limits (Based on the length requirements for inlet and outlet sections, the segment from 16.66m to 21.01m was selected as the test section, meeting uniform flow conditions and minimizing backwater interference from the tailgate.

Table. 2).

Based on the length requirements for inlet and outlet sections, the segment from 16.66m to 21.01m was selected as the test section, meeting uniform flow conditions and minimizing backwater interference from the tailgate.

Table. 2 Test Conditions Table

Relative Water Depth Z1 （H/D）	Channel Constriction Ratio	Bar Spacing	Number of Michelia alba Leaves	Discharge
0.7	0.25	3L	80	22
	0.33	3L	80	
	0.50	3L	80	
1.2	0.33	1.5L	80	28
1.5	0.33	1.5L	80	36
1.8	0.33	1.5L	80	62

An Acoustic Doppler Velocimeter (ADV) was used to measure flow velocity, and a ruler was used to measure water depth. Five verification points were arranged in the test section, located respectively at the center of the upstream area of the shallow-bar and deep-pool, the centers of the upstream and downstream deep pools, and the outer areas, providing data for numerical model validation (Fig. 3).

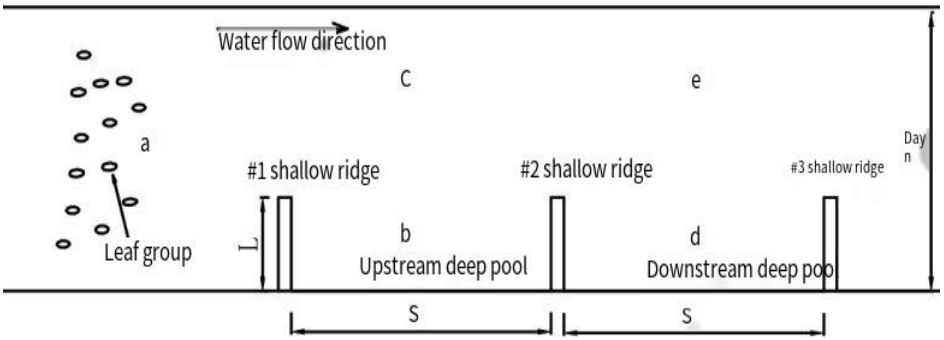

Fig. 3 Schematic Plan of Experimental Setup

A FLOW-3D mathematical model was established to simulate the flume flow field. The model domain was 12m × 2.0m × 0.2m, with a grid size of 0.03m horizontally and refined to 0.01m vertically

2.3.3 Three-Dimensional Flow Field Structure and Leaf Movement Characteristics in the Zhongdui Reach

Condition 1 (channel constriction ratio 0.33, bar spacing 3 times bar length, Z_1=0.7) was used for validation. Results showed that errors in flow velocity and water depth between physical experiments and numerical simulations were less than 5%, indicating the model is scientifically sound (Fig. 4).

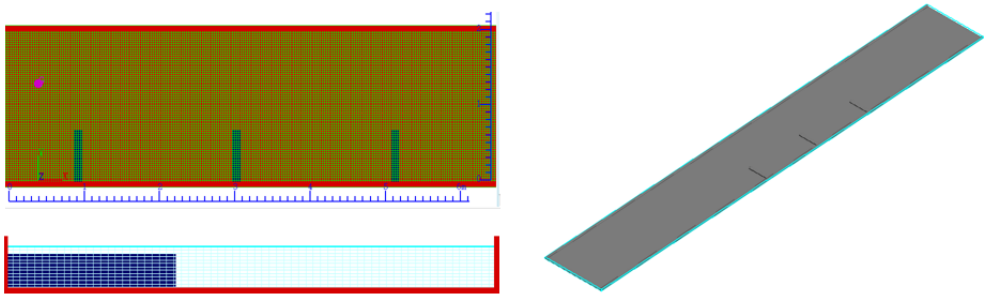

Fig. 4 Mathematical Model Setup Diagram

An oblique shooting method was used to expand the shooting range. Images were later corrected for tilt angle. Tracker software was used to manually track leaf positions, obtaining the coordinates and trajectories of leaves in each frame.Fish schools prefer reef-pool type habitats. Within the Fanshuiqi inner channel, three continuous protruding rock ridges (elevation 150-152m) naturally form a shoal-pool habitat. To avoid affecting ship navigation,

the scheme utilizes dredging and cleared rock debris to heighten and extend the existing rock ridges, constructing three continuous trapezoidal spur dikes (#1, #2, #3) (Fig. 5): lengths 180m, 185m, 170m respectively, crest elevation 153m, crest width 30m, upstream and downstream slopes both 1:3. The aim is to enhance backwater effects, expand low-flow and recirculation zones behind the ridges, and construct continuous shoal-pool habitats suitable for fish. To investigate changes in 3D hydrodynamics and leaf movement before and after scheme implementation, the following methods were used: simulate hydrodynamic characteristics before and after habitat construction using FLOW-3D software; key characteristics like leaf density and settling velocity probability distribution were coded into a Python submodel, then substituted into the Python main model for fluid-structure interaction calculation, ultimately quantifying leaf movement characteristics before and after habitat construction.

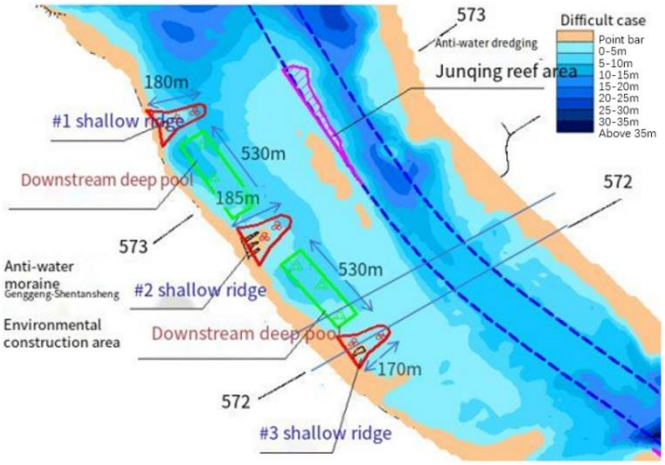

Fig. 5 Schematic Plan of Habitat Creation at the Counter-Current Bar, Zhongdui Reach

The computational domain covered channel kilometers 569–575, with a total length of 6km. A Cartesian grid was used, with a horizontal grid size of 8m, vertical grid size of 2m, totaling 52 layers and approximately 17 million grid cells. The upstream boundary was set as a discharge boundary, and the downstream boundary as a pressure boundary (Fig. 6).

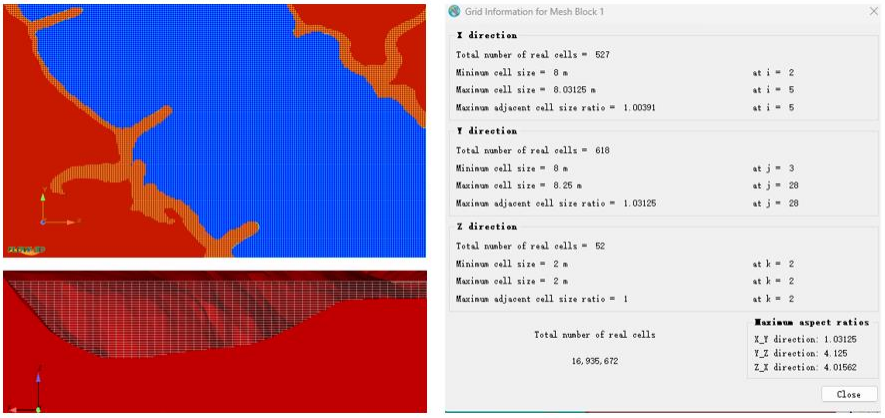

Fig. 6 Grid Division

Seven sets of measured hydrological data (covering drawdown and flood periods) were used for validation. The maximum difference in water level validation was ±0.06m, and flow velocity validation errors were less than 5%. The model calculation results agreed well with measured data, indicating it is suitable for subsequent flow field simulations.

3. Results

3.1 Experimental study outcomes regarding the sedimentation behaviors of fallen leaves

Image processing and manual drawing measured leaf upper surface area; vernier caliper measured thickness; high-precision electronic scale measured weight before soaking and after settling.The results presented in Table 3 indicate that the initial density range of fallen leaves is 0.4-0.9 g/cm³ , concentrated between 0.6~0.8 g/cm³ ; density after settling range 0.7-1.4 g/cm³ , some leaves still had density less than water after settling. Probability distributions of leaf density before soaking and after settling both exhibited normal distribution characteristics.

Table. 3 Changes in leaf density before soaking and after settling

Leaf Type	Characteristics	Initial Weight (g)	Settled Weight (g)	Surface Area (cm²)	Thickness (cm)	Initial Leaf Density	Settled Leaf Density
Cinnamomum camphora leaves	Small, soft texture	0.23	0.36	18.05	0.0253	0.503	0.788
		0.21	0.32	16.5	0.0271	0.469	0.715
Osmanthus fragrans leaves	Round, hard	0.42	0.6	19.75	0.0296	0.718	1.026
		0.81	1.16	38.18	0.0332	0.639	0.915
Photinia serratifolia leaves	Pointed, spiny	0.66	0.92	28.63	0.0285	0.808	1.127
		0.61	0.89	27.75	0.0267	0.823	1.201
Osmanthus fragrans leaves	Pointed, hard, wavy	0.91	1.17	29.38	0.0347	0.892	1.147
		1.08	1.33	33.25	0.0375	0.866	1.066
Ficus microcarpa leaves	Small, soft, thick	0.27	0.34	10.63	0.0331	0.767	0.966
		0.33	0.44	12.63	0.0337	0.775	1.033
Michelia alba leaves	Pale color, slightly curled	0.7	0.86	30.5	0.0301	0.762	0.936
		0.95	1.12	38.88	0.0326	0.749	0.883
Ficus virens leaves	Dark color, flat	0.47	0.64	32.5	0.0211	0.685	0.933
		0.54	0.92	41.5	0.0204	0.637	1.086
Magnolia grandiflora leaves	Hard, flat	0.58	1.18	24.83	0.0341	0.685	1.393
		1.65	2.67	41.18	0.0528	0.758	1.228

Green leaves required longer natural settling time than brown-yellow leaves. Natural leaf settling mainly concentrated in the first week. Larger leaves with more irregular shapes required shorter settling time. Leaf sinking velocity range: 1-4 cm/s. Harder, more irregularly shaped leaves had greater sinking velocities. Sinking velocity probability distribution exhibited log-normal distribution characteristics (Table. 4).

Table. 4 Relevant data of leaf settling

Leaf Type	Characteristics	Initial SubmersionSettling or Not	Days Required for Natural Settling (d)	Settling Process Time (s)	Average Settling Velocity (cm/s)
Cinnamomum camphora leaves	Small, soft texture		21	11.25	1.64
			22	11.84	1.56
Osmanthus fragrans leaves	Round, hard		15	8.66	2.14
			16	9.82	1.88
Photinia serratifolia leaves	Pointed, spiny		5	10.64	1.74
			4	8.8	2.10
Osmanthus fragrans leaves	Pointed, hard, wavy	Yes	2	5.91	3.13
		Yes	1	2.68	3.90
Ficus microcarpa leaves	Small, soft, thick		24		
			23	10.77	1.72
Michelia alba leaves	Pale color, slightly curled		2	9.21	2.01
			1	8.22	2.25

Leaf Type	Characteristics	Initial SubmersionSettling or Not	Days Required for Natural Settling (d)	Settling Process Time (s)	Average Settling Velocity (cm/s)
Ficus virens leaves	Dark color, flat	Yes	3	13.34	1.39
		Yes	3	18.42	1.00
Magnolia grandiflora leaves	Hard, flat		5	7.18	2.58
			4	9.26	2.00

3.2 Results on the Influence of Shoal-Pool Flow Field Structure on Leaf Movement

3.2.1 Leaf Transport Characteristics in Prototype Open Channel Flume

Asynchronous transport refers to the phase of motion where leaf velocity is inconsistent with water flow velocity. During initial release, leaf velocity is 0, fluid resistance is at its maximum, and acceleration is greatest. As leaf velocity increases, fluid resistance gradually decreases, leading to reduced acceleration, until leaf velocity approaches that of the water flow, entering a stage of uniform motion. Numerical simulations and physical experiments have verified that the velocity – time relationship during asynchronous leaf transport follows a power-law pattern: for leaves with a density of 600 kg/m³, $V = 0.14t^{0.24}$; for leaves with a density of 800 kg/m³, $V = 0.097t^{0.412}$. The lower the density, the shorter the asynchronous transport duration; leaves typically complete asynchronous transport within 1–3 s and reach velocity synchronization with the water flow.

In the prototype open channel flume, flow velocity distribution features higher velocities in the center and lower at the sides, causing velocity differences in the water flow around the leaf sides, subsequently forming a pressure difference that pushes leaves towards the central main flow zone.

3.2.2 Influence of Key Factors on Flow Field and Leaf Transport

The shoal-pool zone flow field was divided into main flow zone and recirculation zone (containing positive and negative flow areas) based on streamlines (Fig. 7), and into low-velocity zone (0~0.09 m/s), medium-velocity zone (0.09~0.15 m/s), and high-velocity zone (>0.15 m/s) based on velocity magnitude.

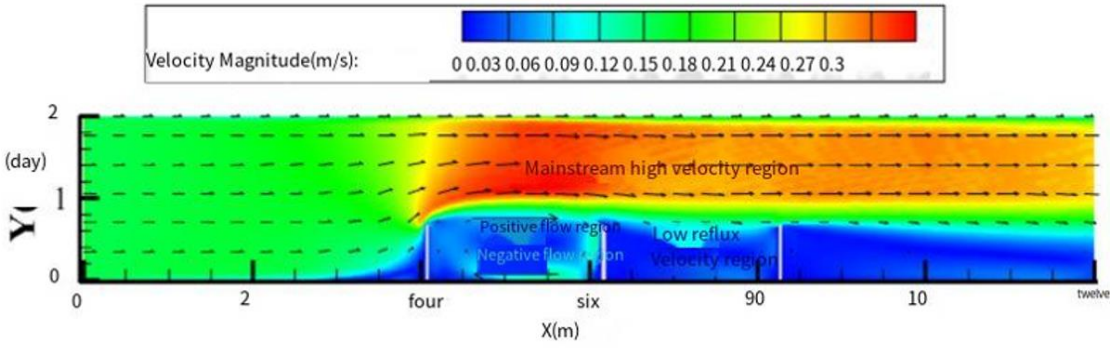

Fig. 7 Schematic diagram of flow field structure division

The effects of the river width contraction ratio on the flow field are as follows: (1) In the velocity field, as the contraction ratio increases, the flow-constructing and damming effects of the shallow ridges are enhanced. The extent of the high-velocity zone in the outer main flow area decreases, but the flow velocity within it increases. Meanwhile, the low-velocity zone in the deep pool expands, and its average velocity rises. Low-velocity zones are concentrated in the deep pool, downstream of #3 shallow ridge, and a small area upstream of #1 shallow ridge, while high-velocity zones are mainly located in the outer main flow and downstream regions. (2) In the recirculation zones, with an increase in the contraction ratio, both the extent and average velocity of the recirculation zones in the upstream and downstream deep pools increase, while the aspect ratio gradually decreases. The upstream deep pool consistently exhibits a larger recirculation zone and higher average velocity than the downstream deep pool, with higher velocities along its edges (Fig. 8). (3) In the turbulent kinetic energy (TKE) field, TKE distributions are similar at contraction ratios of 0.25 and 0.33, but at 0.50, the extent of moderate - to high-TKE zones increases significantly. Moderate- to high-TKE zones are concentrated near the outer sides of the shallow ridges and their downstream areas. The central part of the deep pool evolves toward a low-TKE zone, while its edges develop toward moderate- to high-TKE zones (Fig. 9). (4) In terms of vortex structures, as the contraction ratio increases, the area where vortices appear expands. New vortices mainly emerge in the upstream and downstream deep pools and the main flow zone. Core vortex regions are located along the outer side of the

upstream deep pool, upstream of the base of #1 shallow ridge, and near the head of #3 shallow ridge (Fig. 10).

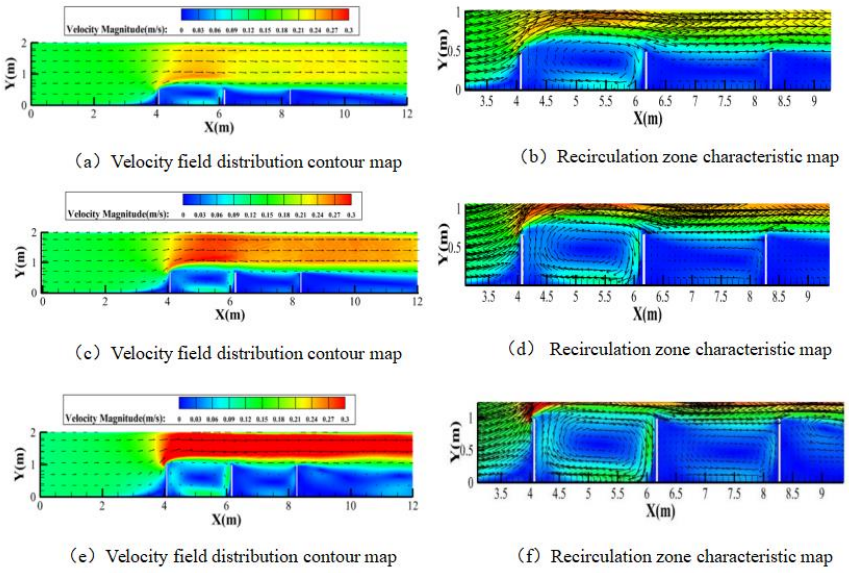

(a) Velocity field distribution contour map (b) Recirculation zone characteristic map

(c) Velocity field distribution contour map (d) Recirculation zone characteristic map

(e) Velocity field distribution contour map (f) Recirculation zone characteristic map

Fig. 8 Velocity field and recirculation zone distribution characteristics under different channel constriction ratios

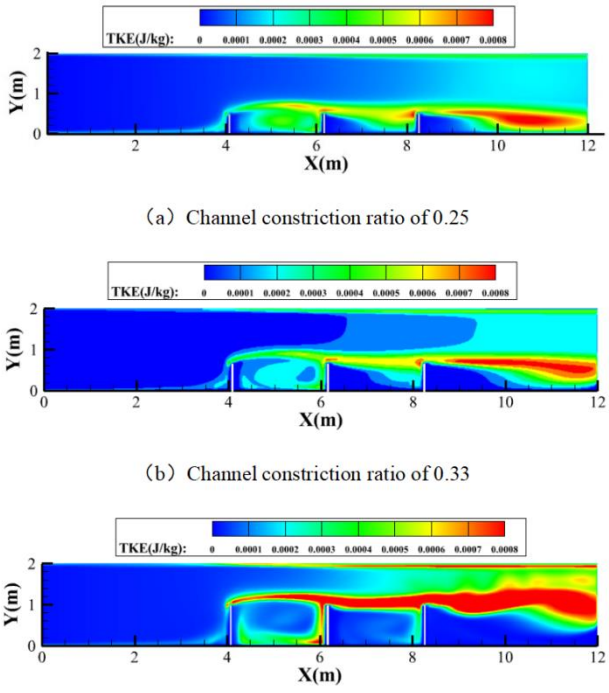

(a) Channel constriction ratio of 0.25

(b) Channel constriction ratio of 0.33

(c) Channel constriction ratio of 0.50

Fig. 9 Turbulent kinetic energy field distribution under different channel constriction ratios

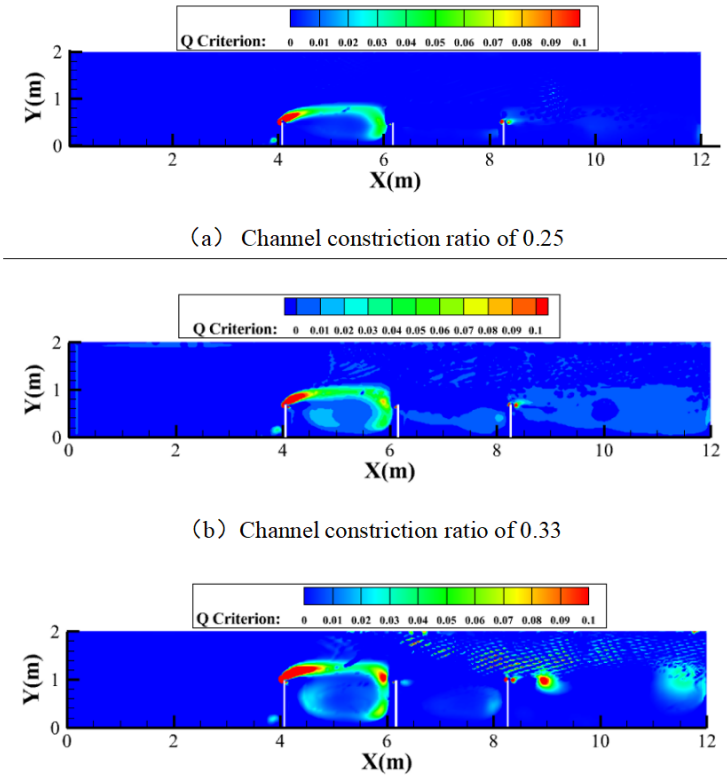

（a） Channel constriction ratio of 0.25

（b） Channel constriction ratio of 0.33

（c） Channel constriction ratio of 0.50

Fig. 10 Vortex structure under different channel constriction ratios

With constriction ratio 0.25, on average only 2 leaves entered the pool. With ratio 0.33, similar numbers entered upstream and downstream pools, average 19 leaves. With ratio 0.50, fewer leaves entered the downstream pool than upstream, average 20 leaves.

The effects of shallow ridge spacing on the flow field are summarized as follows: (1) Regarding the velocity field, when the spacing between shallow ridges is reduced to 1.5L, the sheltering effect of the upstream ridge increases. The mainstream flow is constrained by the downstream ridge before fully developing, resulting in a reduced length of the recirculation zone in the deep pool, with its aspect ratio decreasing to 1.5:1. The variation in velocity contours within the main flow zone is also reduced (Fig. 11). (2) In terms of the turbulent kinetic energy field, at a spacing of 1.5L, the area of high turbulent kinetic energy near the outer region of the deep pool expands, while the average turbulent kinetic energy within the deep pool is relatively low. The similarity in the distribution patterns of turbulent kinetic energy contours is diminished (Fig. 12). (3) As for the vortex structure, at a spacing of 1.5L, the vorticity in the region near the outer part of the upstream deep pool is generally higher, though the overall extent of the vortex zone is limited. Vortices are mainly concentrated in the shallow ridge–deep pool area and in small-scale, low-vorticity eddies downstream (Fig. 13).

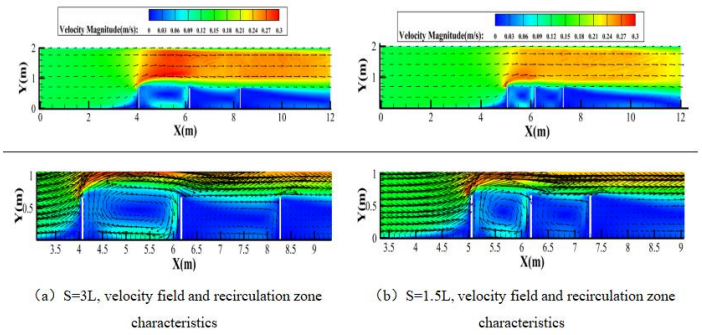

（a） S=3L, velocity field and recirculation zone characteristics

（b） S=1.5L, velocity field and recirculation zone characteristics

Fig. 11 Velocity field and recirculation zone characteristics under different shallow bar spacings

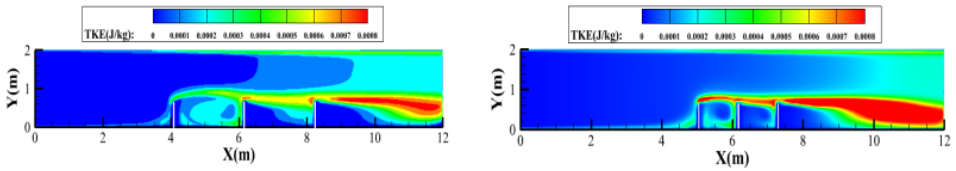

a.S=3L b.S=1.5L

Fig. 12 Turbulent kinetic energy field distribution under different shallow bar spacing

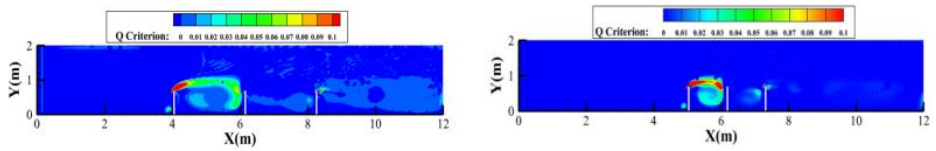

（a）S=3L （b）S=1.5L

Fig. 13 Vortex structure under different shallow bar spacing

At shoal spacing 1.5L, the average number of leaves entering the pool was only 4, far lower than the 3L spacing condition, indicating a recirculation zone length-to-width ratio of 1.5: 1 is unfavorable for leaf entry into the pool.

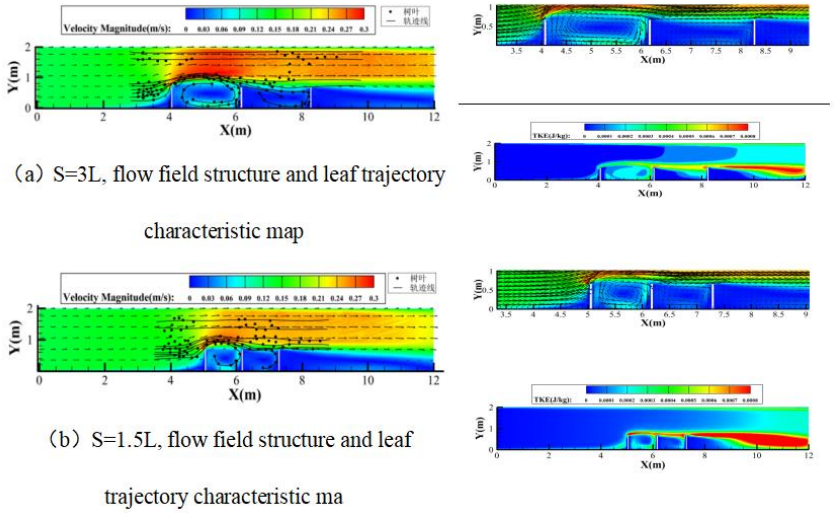

（a）S=3L, flow field structure and leaf trajectory characteristic map

（b）S=1.5L, flow field structure and leaf trajectory characteristic ma

Fig. 14 Flow field structure and leaf trajectory characteristic maps under different shallow bar spacing

The effects of the submergence degree of shallow ridges on the flow field are summarized as follows: (1) Under the condition H/D = 0.7, the flow-constricting effect of the shallow ridges is strong, with the outer mainstream forming a high-velocity zone, while a stable low-velocity recirculation zone develops in the deep pool. The velocity in the upstream deep pool is greater than that in the downstream deep pool. At H/D = 1.2, part of the flow overtops the ridges and enters the deep pool (low velocity), while the rest merges into the outer high-velocity mainstream. The velocity near the ridge crests is relatively high, and a recirculation zone with a height similar to that of the ridges forms downstream. At H/D = 1.5, the flow-constricting and plunging effects of the ridges weaken, leading to increased velocity in the deep pool and a slight decrease in the mainstream velocity. The streamlines become smoother, with no significant changes in the characteristics of the recirculation zone. At H/D = 1.8, the influence of the ridges is minimal. The surface velocity generally increases with straighter streamlines, no distinct recirculation zone is observed, the velocity difference between the mainstream and the deep pool narrows, and the velocity distribution becomes more uniform (Fig. 15). (2) Regarding the turbulent kinetic energy (TKE) field: Under shallow submergence (H/D = 1.2), the flow pattern around #1 shallow ridge becomes most disturbed (Fig. 16), resulting in the highest TKE. Under moderate submergence (H/D = 1.5), the velocity slightly decreases, and TKE drops significantly. Under deep submergence (H/D = 1.8), velocity increases, and TKE generally rises, with

the shallow ridge–deep pool area predominantly consisting of high-turbulence zones. (3) Regarding the vortex structure:Under shallow submergence, the extent and vorticity of vortices formed over the ridge crests decrease sequentially. Vortices mainly develop in the outer mainstream of the downstream deep pool and its farther downstream areas. Under moderate submergence, both the vortex extent and vorticity further decrease. Under deep submergence, the vortex extent and vorticity above the ridges become very small, while large-scale, high-vorticity vortices form in the mainstream and its downstream region (Fig. 17).

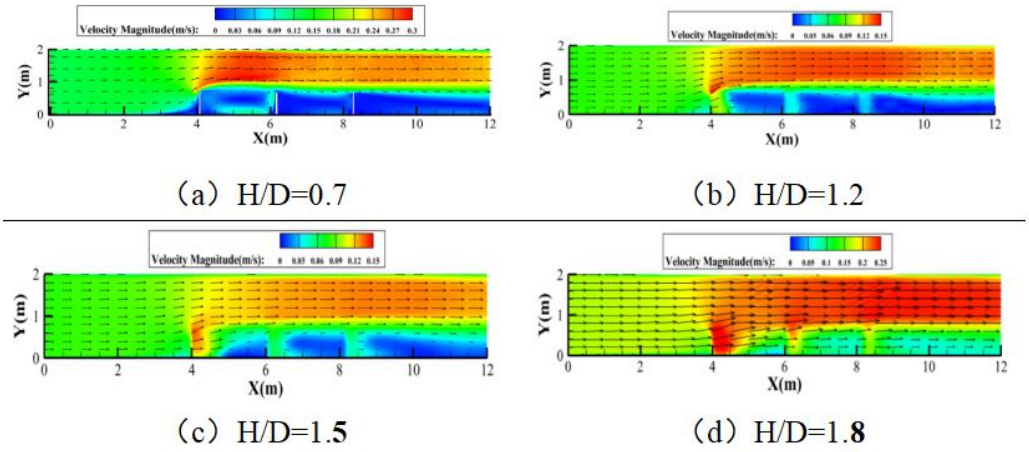

Fig. 15 Velocity line variation characteristics under different shallow bar submergence degrees

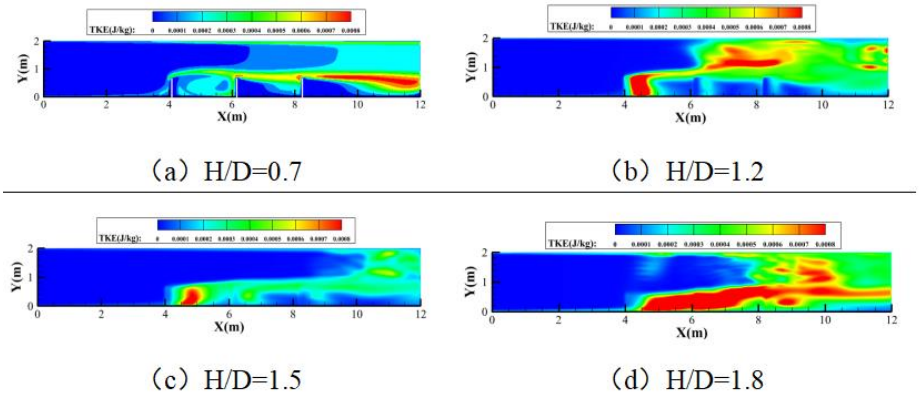

Fig. 16 Turbulent kinetic energy field distribution under different shallow bar submergence degrees

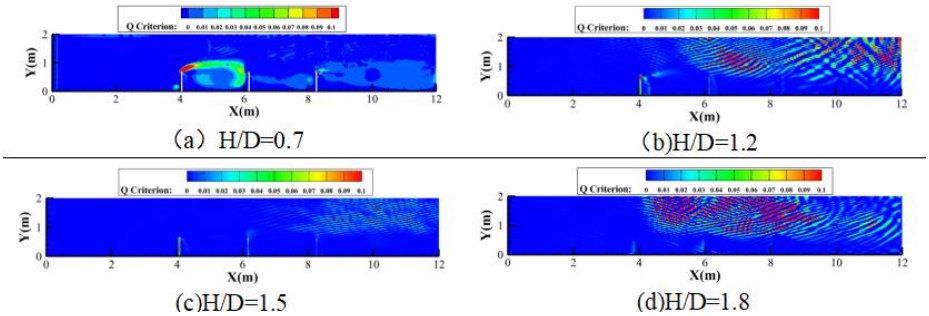

Fig. 17 Vorticity field distribution under different shallow bar submergence degrees

After shoal submergence, leaves are not drawn into the pool by plunging flow (Fig. 18). As submergence increases, shoal influence on leaf transport decreases, and the probability of leaves passing completely through the shoal-pool increases. H/D=1.2: Upstream pool average 10 leaves, 6 enter downstream pool. H/D=1.5: Upstream pool 16 leaves, 7 enter downstream pool. H/D=1.8: Upstream pool 33 leaves, 23 enter downstream pool (Table.

5).

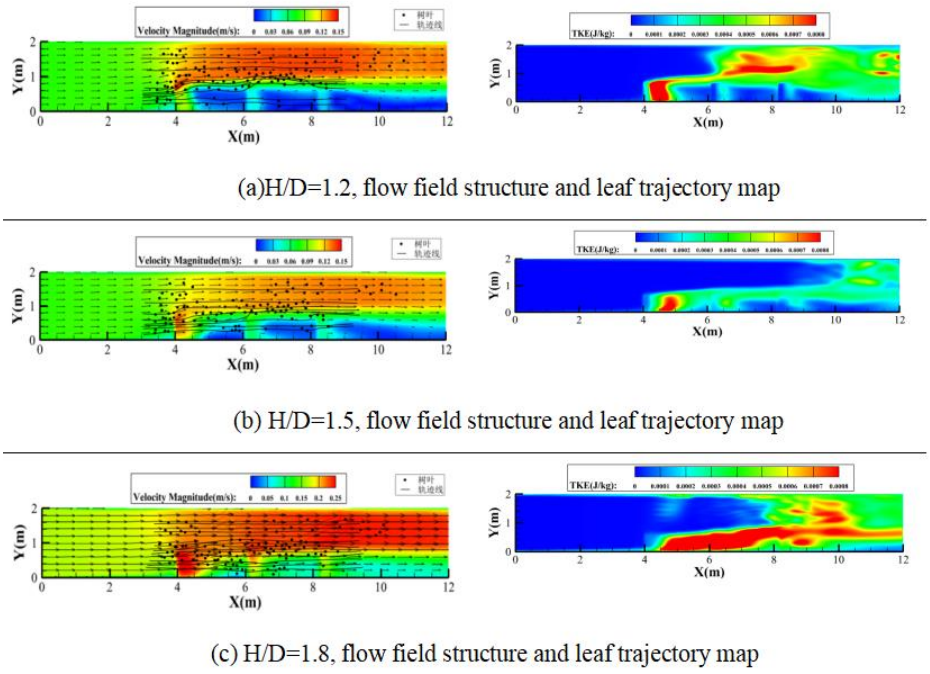

(a)H/D=1.2, flow field structure and leaf trajectory map

(b) H/D=1.5, flow field structure and leaf trajectory map

(c) H/D=1.8, flow field structure and leaf trajectory map

Fig. 18 Flow field structure and leaf trajectory maps under different shallow bar submergence degrees

Table. 5 Number of leaves entering the deep pool under each working condition

Channel Constriction Ratio	Shallow Bar Spacing	Number of Michelia alba Leaves (pieces)	Discharge (L/S)	Number of Leaves Entering the Deep Pool Each Time (pieces)	Average Number of Leaves Entering the Deep Pool (pieces)
0.25	3L	80	22	1、3、1、0、4	2
0.33	3L	80		19、17、21、19、18	19
0.50	3L	80		19、21、23、17、21	20
0.33	1.5L	80		5、2、2、4、6	4
0.33	1.5L	240	28		
0.33	1.5L	240	36	0	0
0.33	1.5L	240	62		

3.3 Simulation results of the river reach case study

3.3.1 Characteristics of Flow Field Structure Changes

In the surface flow velocity field, the overall patterns before and after the project implementation are similar. The flow first contracts and then expands abruptly at the gorge entrance, with higher velocities observed near the thalweg. After the project, the extent of the recirculation zone in the shallow ridge-deep pool area at the backwater riffle increases significantly during the drawdown period, while the flow-constructing effect of the shallow ridge is enhanced during the flood season, resulting in a straighter flow direction in the navigation channel [9].

In the vertical velocity field, after the project implementation, the average vertical flow velocities decrease along the right bank and increase along the left bank. Velocity generally decreases from the left bank to the right bank and increases from the bottom to the surface. The average vertical flow velocity in the upstream deep pool is higher than that in the downstream deep pool (Fig. 19).

In the surface turbulent kinetic energy field, turbulent kinetic energy increases significantly with discharge, with higher values observed near the gorge entrance, shallow ridges, and reefs. After the project implementation,

turbulent kinetic energy increases in the gorge entrance and the shallow ridge-deep pool area.

In the vertical turbulent kinetic energy field, under the same discharge condition, the average turbulent kinetic energy in the upstream deep pool is slightly higher than that in the downstream deep pool. After the project, the average turbulent kinetic energy across all cross-sections is slightly greater than before the project. As discharge increases, turbulent kinetic energy in all cross-sections rises significantly (Fig. 20).

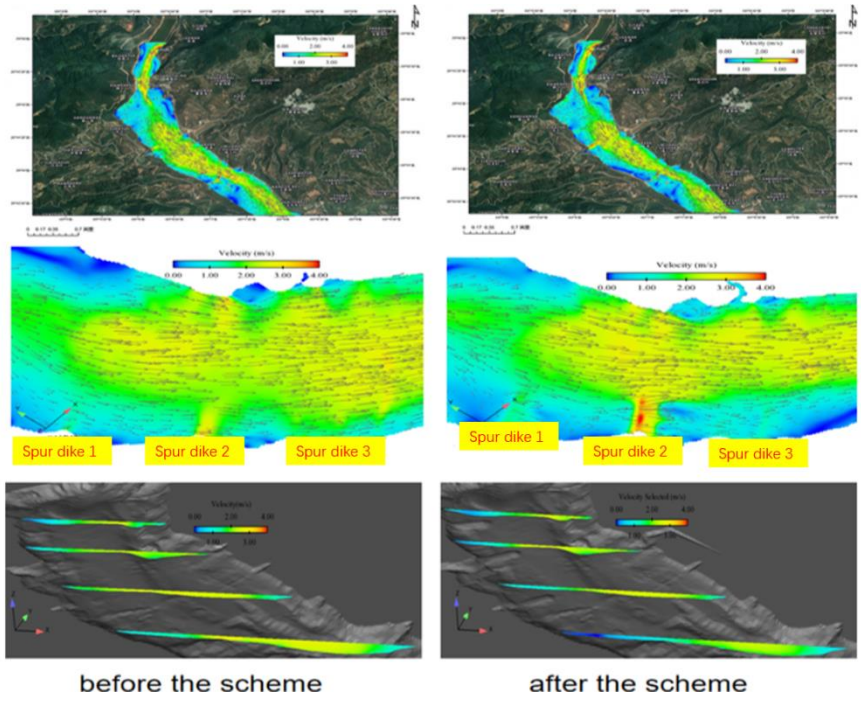

Fig. 19 Diagram of variations in the flow velocity field before and after the scheme

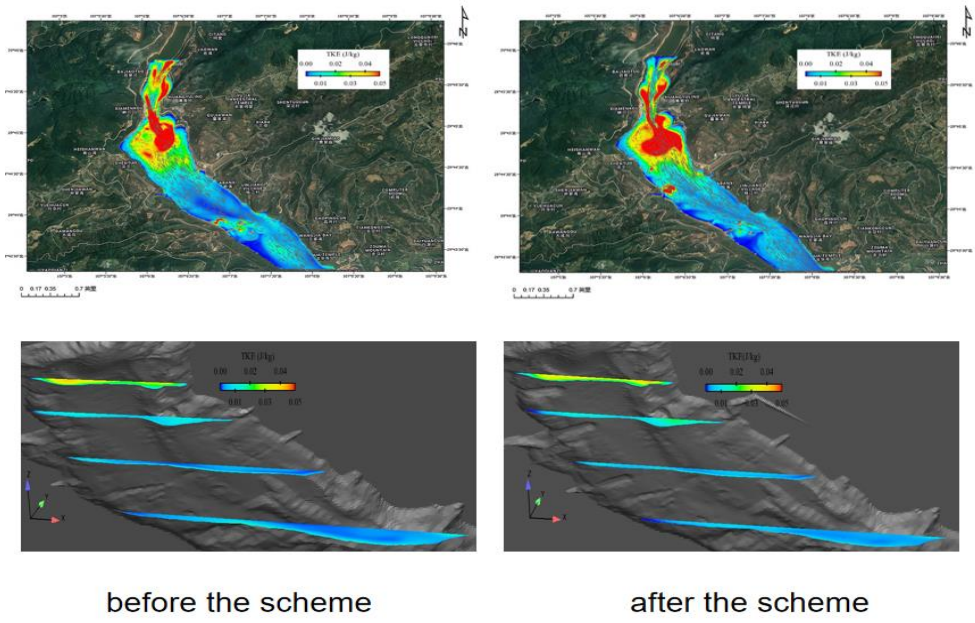

Fig. 20 Diagram of variations in the stored kinetic energy field before and after the scheme

3.3.2 Characteristics of Leaf Movement Trajectories

In the validation of the Lagrangian model, the optimal condition from the flume test was used to verify the Lagrangian leaf tracking model. The results showed that the leaf distribution characteristics were consistent with

the experimental data, indicating good model simulation performance. Regarding the leaf movement trajectories, leaves were released in the sudden expansion area downstream of the gorge entrance. Some were retained by the recirculation zones, while others circled before entering the shoal-pool area. Before the scheme implementation, leaves primarily moved along areas with higher turbulent kinetic energy (TKE). After the scheme, leaves tended to move along the high-TKE zones outside the shoal-pool, with some entering and being retained in the pools, which aligns with the conclusions from the flume experiments. Concerning the leaf distribution state, leaves in the river exhibited an overall parabolic distribution, with the peak concentration in the mid-channel and the endpoints near both banks. During the drawdown period, the probability of leaves being retained in the pools after the scheme implementation was significantly greater than before. This is related to the expansion of the recirculation zones and the increase in turbulent kinetic energy within the shoal-pool area (Fig. 21Fig. 22).

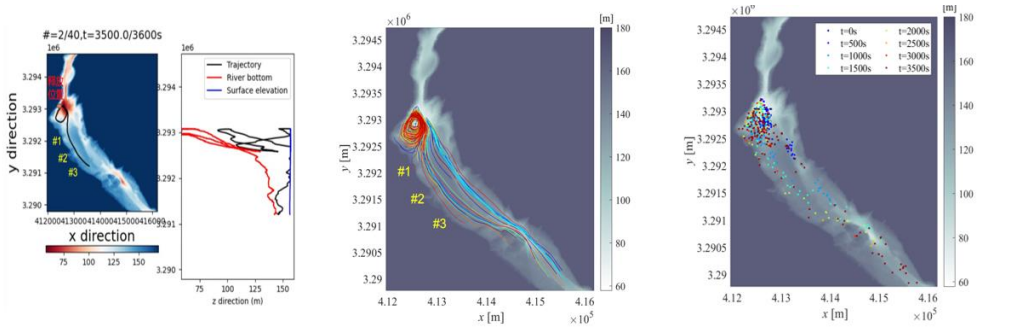

(a)Detailed trajectory characteristics of a single leaf

(b)Trajectory characteristics of multiple leaves

(c)Planar distribution characteristics of multiple leaves at different time instants

Fig. 21 Diagram of leaf trajectory distribution before the scheme

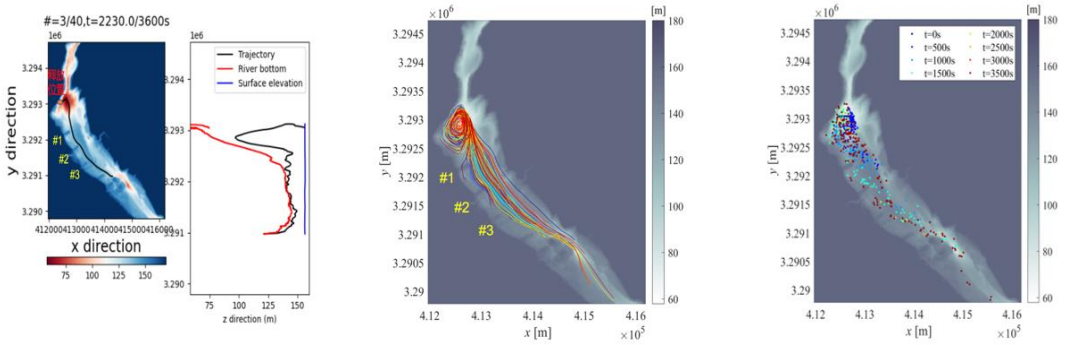

(a)Detailed trajectory characteristics of a single leaf

(b)Trajectory characteristics of multiple leaves

(c)Planar distribution characteristics of multiple leaves at different time instants

Fig. 22 Diagram of leaf trajectory distribution after the scheme

4. Discussion

4.1 Leaf Settling Behaviors

This experiment revealed that the settling behavior of leaves in water is not governed by density alone, but results from the synergistic effects of surface wettability, shape structure, chemical composition, and density. Some leaves ultimately sank despite having post-settlement densities (0.7-0.9 g/cm³) lower than that of water. The core mechanism lies in the gradual expulsion of air from the leaf stomata during immersion, which increases the effective density of the leaf blade. Simultaneously, water absorption wets the leaf surface, significantly reducing the surface tension acting upon it. Settlement is triggered when the gravitational force exceeds the sum of the residual surface tension and buoyancy. This finding supplements and deepens the traditional hydraulic framework that primarily relies on a density threshold to determine the buoyancy of objects. It aligns in physical mechanism with the "porous medium water absorption-air expulsion" settlement initiation model proposed by Heer in their simulation of grass carp egg transport, suggesting common physical processes in the settling behavior of biological organic particles across different materials and scales[10].

The measured initial density of leaves ranged from 0.4 to 0.9 g/cm³, mostly concentrated between 0.6~0.8 g/cm³, which is generally lower than the density of water. The post-settlement density range increased to 0.7-1.4 g/cm³, although some leaves remained below 1.0 g/cm³ even after settling. This directly confirms that density is not the sole determinant of leaf settlement. The posture of leaves in water and their intrinsic characteristics significantly influence their force balance and trajectory. In their study of leaf decomposition processes in streams, it observed phenomena that align with this conclusion: the physical structure of leaves (e.g., hardness, vein morphology) is a key factor regulating their early retention and positioning in water bodies, rather than being limited solely to leaf density.

The sinking velocities of different leaves showed significant variation: harder, irregularly shaped leaves sank faster, reaching 3.13~3.90 cm/s; whereas softer, more regularly shaped leaves sank slower, at only 1.56~1.64 cm/s. This difference stems mainly from two aspects: First, irregular shapes may reduce the form drag experienced during settling, consistent with the view pointed out by May in a review that "particle morphology has a critical influence on its transport rate in the water column[11]." Second, the cellular structure of harder leaves may allow for faster water saturation, leading to a more rapid and significant increase in density, thereby accelerating settlement. This is intrinsically linked to the finding by Duan in their study on the decomposition dynamics of aquatic plants that "material structural rigidity affects the initial leaching and physical fragmentation rate [12], [13]."

Furthermore, a quantitative difference exists in the time required for natural settlement between evergreen plant leaves and deciduous plant leaves (21~24 days for the former versus only 1~5 days for the latter). The underlying cause is the difference in water absorption efficiency regulated by leaf cuticle thickness. Evergreen leaves typically possess a thicker cuticle, effectively slowing water infiltration into the cells and thus significantly prolonging their floating period.

4.2 Influence of Shoal-Pool Flow Field Structure on Leaf Movement

This study found that the flow field structure in the shallow ridge-deep pool area, particularly the characteristics of the recirculation zone, the distribution of turbulent kinetic energy, and the vortex dynamics, directly regulates the transport pathways and final accumulation efficiency of leaves. This process is primarily controlled by three key hydraulic parameters: the river width contraction ratio, the spacing between shallow ridges, and the degree of submergence.

The width contraction ratio significantly influences the mainstream velocity, the turbulent kinetic energy level in the outer region, and the development morphology of the recirculation zone within the deep pool by altering the flow-constricting intensity of the shallow ridges. When the contraction ratio was 0.33, the turbulent kinetic energy of the flow outside the shallow ridge-deep pool area was observed to be within a moderate range (0.0003~0.0007 J/kg), while the length-to-width ratio of the recirculation zone formed in the deep pool was approximately 3:1. Under these conditions, the probability of leaves entering the deep pool was the highest (average 19 leaves per group). The essence of this optimal condition lies in achieving a balance between "turbulent diffusion driving lateral transport" and "effective capture and retention by the recirculation zone structure." Moderate turbulent kinetic energy enhances lateral mixing and momentum exchange in the flow, helping to guide leaves from the mainstream area towards the edge of the deep pool. The 3:1 recirculation zone structure provides sufficient space and appropriate flow patterns, allowing leaves to enter and be retained within the relatively low-velocity deep pool, rather than being carried away by the high-velocity mainstream. These results align with the findings of Chen regarding the division of recirculation zone structures in continuous spur dikes and their energy exchange with the mainstream, which also emphasized the crucial role of recirculation zone geometry on material exchange efficiency [1]. When the contraction ratio increased to 0.50, although the local turbulent kinetic energy outside the shallow ridges further intensified (>0.0008 J/kg), the length-to-width ratio of the recirculation zone decreased to 2:1. Its structure became "shorter and wider," and its capacity for leaf capture and retention did not improve proportionally . Conversely, when the contraction ratio decreased to 0.25, the recirculation zone was underdeveloped and the turbulent kinetic energy was weak, making it nearly impossible for leaves to enter the deep pool . This confirms that for floating matter like leaves with specific dynamic responses, the integrity of the flow field structure (especially the effective volume and morphology of the recirculation zone) is more critical than the degree of flow turbulence alone.

The spacing between shallow ridges is another core parameter determining the flow interaction between adjacent ridges and the morphology of the deep pool recirculation zone. Experiments showed that when the spacing was reduced to 1.5 times the shallow ridge length (S = 1.5L), the energy exchange between the vortices generated by the upstream ridge and the mainstream, before fully developing, was constrained by the downstream ridge. This resulted in similar morphologies and significantly reduced length-to-width ratios (approximately 1.5:1) of the recirculation zones in both upstream and downstream deep pools, leading to a sharp decrease in the number of leaves entering the deep pools (average 4 leaves per group). This indicates that overly small spacing inhibits the full development of the recirculation zone and is detrimental to leaf capture. By comparing experimental data

under different combinations of contraction ratios and spacings, it was found that the leaf accumulation effect was optimal when the recirculation zone length-to-width ratio was approximately 3:1 (corresponding to the condition of 0.33 contraction ratio and S = 3L). This optimal spacing relationship is inherently consistent with the empirical range proposed by Jowett based on observations of natural river geomorphology, that "habitat structure is most stable when the alternating wavelength of shallow bars and deep pools is about 2.2~5 times the river width [14]." This study extends this geomorphological concept to the hydrodynamic design of artificial habitats, clarifying that a spacing around 3 times the dike length (under the experimental width contraction ratio of 0.33, S = 3L corresponds to approximately 3.3 times the contracted river width) can form a hydraulically efficient "guidance-retention" structure, thereby optimizing the accumulation function for floating organic matter.

The degree of submergence profoundly alters the flow structure and its interaction with leaves. When the shallow ridges are not submerged, clear flow separation and stable recirculation zones form the basis for leaves to enter and be retained in the deep pool. Once the shallow ridges are submerged, where water flows over the crest, it becomes difficult to maintain a typical recirculation zone structure in the deep pool area. Simultaneously, the plunging process over the ridge crest generates a downward flow component, rather than the lateral velocities conducive to drawing floating objects into the deep pool. This experiment observed that in the submerged state, leaves tended to follow the mainstream in surface areas with higher turbulent kinetic energy and were difficult to retain in the deep pool. As the degree of submergence (H/D) increased from 1.2 to 1.8, the influence of the shallow ridge topography on leaf movement continuously diminished. This is consistent with the conclusion of Bai, revealed through Large Eddy Simulation regarding the flow characteristics around submerged spur dike groups-namely, that the disturbance of the dike body on the surface flow weakens with increasing relative water depth [2]. This finding is significant for habitat management, implying that during high-water periods in flood season, the function of accumulating surface floating organic matter relying on the shallow ridge-deep pool structure will significantly attenuate.

Based on the above analysis of flow field mechanisms and using the "probability of leaves entering the deep pool" as a key indicator for evaluating the organic matter accumulation function of shallow ridge-deep pool habitats, this study proposes that a width contraction ratio of 0.33 combined with a shallow ridge spacing of S = 3L (approximately 3 times the dike length) can serve as an optimized parameter combination for constructing such habitats. This design, while ensuring navigation conditions for vessels and meeting the suitable flow velocity requirements for fish , can maximize the capture efficiency of floating organic matter like leaves. In engineering practice, if conditions permit, appropriately increasing the height of the shallow ridges could be considered to delay their submergence time, thereby maintaining their effective organic matter accumulation function over a longer hydrological year. This provides a quantitative hydraulic basis for the refined design of habitats in ecological waterway construction.

4.3 Ecological Implications

The core value of this study lies in revealing the ecological chain of "shoal-pool flow field optimization – leaf enrichment – fish nutrient supply," providing key technical support and theoretical basis for green ecological waterway construction in the upper Yangtze River.

From a habitat construction perspective, the optimal scheme (constriction ratio 0.33, shoal spacing 3 times shoal length) ensures leaf aggregation effectiveness while avoiding the risk of soil and rock loss from excessive spur dike extension. It also does not affect ship navigation or other suitability indicators for fish habitats, providing a scientific reference for ecological waterway construction in the upper Yangtze and similar river reaches. The implementation of this scheme increases the average turbulence energy in the reach during both drawdown and flood periods, significantly expands the recirculation zone extent in upstream and downstream pools, and increases turbulence near the shoal-pool outer areas, more conducive to leaf retention in the pools, thereby providing richer nutrients for fish. This achieves coordination between navigation development and ecological protection, holding significant meaning for enhancing river ecosystem functions and protecting biodiversity.

From an engineering practice perspective, the research clarifies the ecological functional boundaries of shoal-pool habitats: nutrient enrichment function is optimal under non-submerged conditions; under submerged conditions, enrichment effectiveness needs to be maintained by adjusting shoal height (appropriately increasing it), providing targeted schemes for habitat construction under different hydrological conditions. Simultaneously, the coupling relationship between leaf settling characteristics and flow field parameters provides a quantitative basis for the refined design of habitat construction.

In summary, through the combination of physical experiments and numerical simulation, this study clarifies the multi-factor synergistic mechanism of leaf settling, reveals the regulatory patterns of shoal-pool flow field structures on leaf movement, and proposes habitat construction schemes with both ecological benefits and engineering feasibility. The research results not only provide direct technical support for ecological protection in the upper Yangtze waterway construction but also offer important references for practical pathways in ecological restoration of other rivers.

5. Conclusion

This study demonstrates that leaf sedimentation in riverine environments is controlled by the combined effects of surface wettability, morphological structure, chemical composition, and density, rather than density alone. The measured initial leaf density ranged from 0.4 – 0.9 g/cm³ and increased to 0.7 – 1.4 g/cm³ after settling, with sinking velocities between 1 – 4 cm/s. Harder and more irregularly shaped leaves settled faster, while evergreen leaves exhibited prolonged floating periods. These findings provide essential parameters for hydrodynamic – biological coupling simulations.

The research further clarifies how riffle-pool flow structures regulate leaf transport and identifies an optimal hydraulic configuration-channel constriction ratio of 0.33, riffle spacing of three times the riffle length (3L), and non-submerged conditions-that maximizes organic matter retention. This configuration achieves a balance between turbulent diffusion and recirculation zone capture, forming an efficient "flow – transport – accumulation" pathway.

Application of the optimized scheme to the Zhongdui reach in the Upper Yangtze River verified its ecological and engineering effectiveness: recirculation zones expanded, navigation alignment improved, leaf retention probability increased, and risks of soil and rock loss were mitigated. These results provide a replicable technical framework for constructing green ecological waterways in mountainous navigable rivers.

This work offers a systematic elucidation of the capture mechanism of floating organic debris by riffle – pool habitats and proposes quantitative design parameters for integrated ecological waterway construction. Future research should determine the optimal nutrient accumulation levels required to support fish growth and ecosystem functioning [15].

CRediT authorship contribution statement

Geng Li: Writing-review & editing, Writing-original draft, Visualization, Investigation, Formal analysis, Data curation, Conceptualization. **Jianzhuang Chen**: Writing-review & editing, Supervision, Resources, Conceptualization. **Jianghua Liao**: Writing-review & editing, Funding acquisition. **Jiang Hu**: Writing-review & editing, Investigation, Conceptualization. **Shengfa Yang**: Writing-review & editing, Investigation, Conceptualization.

Declaration of competing interest

We have nothing to declare.

Acknowledgments

The authors would like to thank the anonymous referees and editors for their careful work and constructive suggestions. This work was supported by the China Postdoctoral Science Foundation (Grant No. 2024M763880) and the Chongqing Postdoctoral Special Support (Grant No. 2023CQBSHTB3061).

6. References

[1] Chen Z., Hei PF, and Ding X, 'Experimental study on turbulence intensity in the recirculation zone of spur dikes', *J Tsinghua Univ Sci Technol*, vol. 48, no. 12, pp. 2053–2056, 2008, doi: 10.16511/j.cnki.qhdxxb.2008.12.011.

[2] Bai J., Fang HW, and He GJ, 'Three-dimensional large eddy simulation of flow around non-submerged spur dikes', *Acta Mech Sin*, vol. 45, no. 2, pp. 151–157, Mar. 2013, doi: 10.6052/0459-1879-12-309.

[3] Yang J., Zhang MY, Feng JC, and Liu YM, 'Study on sediment carrying capacity in the recirculation zone downstream of spur dikes considering flow turbulence', *Minzu Univ China Nat Sci Ed*, vol. 0, no. 2, pp. 53–57, 2016.

[4] D. C. Steart, P. I. Boon, D. R. Greenwood, and N. T. Diamond, 'Transport of leaf litter in upland streams of Eucalyptus and Nothofagus forests in south-eastern Australia', *Arch. Für Hydrobiol.*, vol. 156, no. 1, pp. 43–61, Dec. 2002, doi: 10.1127/0003-9136/2002/0156-0043.

[5] H. Xu, M. Zhang, and W. Q. Zhang, 'Three-Dimensional Flow Simulation Research on Spur Dike', *Appl. Mech. Mater.*, vol. 405–408, pp. 799–802, Sept. 2013, doi: 10.4028/www.scientific.net/AMM.405-408.799.

[6] G. Li and B. Wang, 'Simulation of the flow field and scour evolution by turbulent wall jets under a sluice gate', *J. Hydro-Environ. Res.*, vol. 43, pp. 22–32, July 2022, doi: 10.1016/j.jher.2022.06.002.

[7] M. Ghodsian and M. Vaghefi, ‘Experimental study on scour and flow field in a scour hole around a T-shape spur dike in a 90° bend’, *Int. J. Sediment Res.*, vol. 24, no. 2, pp. 145–158, June 2009, doi: 10.1016/ S1001-6279(09)60022-6.

[8] Fazli M., Ghodsian M., and Neyshabouri S. A. A. S., ‘Scour and flow field around a spur dike in a 90° bend’, International Journal of Sediment Research, vol. 23, no. 1, pp. 56–68, 2008.

[9] N. Nagata, T. Hosoda, T. Nakato, and Y. Muramoto, ‘Three-Dimensional Numerical Model for Flow and Bed Deformation around River Hydraulic Structures’, *J. Hydraul. Eng.*, vol. 131, no. 12, pp. 1074–1087, Dec. 2005, doi: 10.1061/(ASCE)0733-9429(2005)131:12(1074).

[10] T. Heer, M. G. Wells, P. R. Jackson, and N. E. Mandrak, ‘Modelling grass carp egg transport using a 3-D hydrodynamic river model: the role of egg retention in dead zones on spawning success’, *Can. J. Fish. Aquat. Sci.*, vol. 77, no. 8, pp. 1379–1392, Aug. 2020, doi: 10.1139/cjfas-2019-0344.

[11] C. L. May and B. S. Pryor, ‘Initial motion and bedload transport distance determined by particle tracking in a large regulated river’, *River Res. Appl.*, vol. 30, no. 4, pp. 508–520, May 2014, doi: 10.1002/rra.2665.

[12] J. G. Duan, L. He, X. Fu, and Q. Wang, ‘Mean flow and turbulence around experimental spur dike’, *Adv. Water Resour.*, vol. 32, no. 12, pp. 1717–1725, Dec. 2009, doi: 10.1016/j.advwatres.2009.09.004.

[13] J. Shim and J. G. Duan, ‘Experimental study of bed-load transport using particle motion tracking’, *Int. J. Sediment Res.*, vol. 32, no. 1, pp. 73–81, Mar. 2017, doi: 10.1016/j.ijsrc.2016.10.002.

[14] I. G. Jowett, ‘A method for objectively identifying pool, run, and riffle habitats from physical measurements’, *N. Z. J. Mar. Freshw. Res.*, vol. 27, no. 2, pp. 241–248, June 1993, doi: 10.1080/00288330. 1993.9516563.

[15] Gu JY, Lu YJ, Liu HX, Tan YN, Huang TJ, and Duan GL, ‘Evolution Characteristics of Flow and Sediment in Pool-Riffle Sequences on a Gravel-Bed River of the Dongjiang River’, *Adv. Water Sci.*, vol. 33, no. 1, pp. 111–122, 2022, doi: 10.14042/j.cnki.32.1309.2022.01.011.